
Connecting adversarial attacks and optimal transport for domain adaptation

Arip Asadulaev
 ITMO University
 Artificial Intelligence Research Institute
 aripasadulaev@itmo.ru

Vitaly Shutov
 ITMO University
 VK
 vi.shutov@corp.vk.com

Alexander Korotin
 Skolkovo Institute of Science and Technology
 Artificial Intelligence Research Institute
 a.korotin@skoltech.ru

Alexander Panfilov
 Eberhard Karls Universität Tübingen
 kotekjedi@gmail.com

Andrey Filchenkov
 ITMO University
 afilchenkov@itmo.ru

Abstract

We present a novel algorithm for domain adaptation using optimal transport. In domain adaptation, the goal is to adapt a classifier trained on the source domain samples to the target domain. In our method, we use optimal transport to map target samples to the domain named *source fiction*. This domain differs from the source but is accurately classified by the source domain classifier. Our main idea is to generate a *source fiction* by c -cyclically monotone transformation over the target domain. If samples with the same labels in two domains are c -cyclically monotone, the optimal transport map between these domains preserves the class-wise structure, which is the main goal of domain adaptation. To generate a *source fiction* domain, we propose an algorithm that is based on our finding that adversarial attacks are a c -cyclically monotone transformation of the dataset. We conduct experiments on Digits and Modern Office-31 datasets and achieve improvement in performance for simple discrete optimal transport solvers for all adaptation tasks.

1 Introduction

Optimal Transport (OT) is a simple framework for solving mass-moving problems for probability distributions. Optimal transport was successfully applied in mathematics [13], economics [51], and machine learning [2, 38, 59, 6], especially in domain adaptation (DA) problem [7, 45, 48]. The discrete OT algorithms for DA are used to map the labeled source samples to the unlabeled or partially labeled samples in the target domain.

The optimal transport results in domain adaptation depend on the cost function c (§2). The optimal transport aims to find a c -cyclically monotone [36] map; it is impossible to perturb such a map and get a more cost-efficient one [63]. However, a cyclically monotone map with Euclidean cost may incorrectly capture the class-wise structure between domains, leading to inaccuracy of domain adaptation by optimal transport.

To correctly capture the class-wise structure during domain adaptation via optimal transport, we present a novel algorithm that maps the target to the domain named *source fiction*. The *source fiction*

domain differs from the real source but it is also **classified correctly** by the source classifier. At the same time, mapping the target to the *source fiction* (by OT with Euclidean cost) **saves the class-wise structure**.

To generate the *source fiction*, we propose to use the c -cyclically monotone transformation of the target domain. The idea is that if we transform the target by c -cyclically monotone map, then the corresponding sample in the *source fiction* will have the same label. More details about c -cyclical monotonicity see in Section (§2.1.1)

As the c -cyclically monotone transformation that makes target samples classified correctly by the source classifier, we propose to use an adversarial attack [60]. We demonstrate that Iterative Fast Sign Gradient Descent (FSGD) [17] is a c -cyclically monotone transformation over the dataset with quadratic cost. In other words, we replace the source domain with a new domain constructed by the gradients of the source classifier over the target samples. It is important to note that in our method, the adversarial attack turns samples into the correctly classified instead of "fooling" classifier, hence we call it *inverse adversarial attack*. It is necessary to have some labeled samples in the target domain to apply an inverse adversarial attack. Therefore, our method is semi-supervised.

In our experiments, we show that in semi-supervised settings, our method improves the accuracy of discrete OT solvers on a range of DA tasks (§5.4). The improvement of discrete OT solvers is important, as this method has low complexity and solves DA faster than the deep neural network-based DA algorithms [15, 33, 18, 32, 34].

Contribution: We propose a novel method for semi-supervised domain adaptation with optimal transport. We prove that adversarial attacks are a c -cyclically monotone transformation of the dataset (§4.1). Using this property, we propose a novel algorithm that improves the performance of the OT solvers on the range of DA problems (§5).

2 Background

2.1 Optimal transport

OT can be a simple solution for the domain adaptation problem. OT aims at finding a cost-effective mapping $T : X \rightarrow Y$ of the two probability measures $\mathbb{P} = \sum_{i=1}^n a_i x_i$ and $\mathbb{Q} = \sum_{j=1}^m b_j y_j$ with respect to the cost function $c : X \times Y \rightarrow \mathbb{R}_+$, where a_i and b_i are the values of the Dirac function at x_i and y_j correspondingly. Monge's problem was the first example of the OT problem [63, §3] and can be formally expressed as follows:

$$\inf_{T \# \mathbb{P} = \mathbb{Q}} \int_{\Omega_p} c(\mathbf{x}, T(\mathbf{x})) \mathbb{P}(\mathbf{x}) d\mathbf{x} \quad (1)$$

Monge's formulation of OT aims at finding a map T where $T \# \mathbb{P}_s = \mathbb{Q}_t$ represents the mass preserving push forward operator. In Monge's formulation, for two given measures \mathbb{P} and \mathbb{Q} , the existence of a transport map T is not only non-trivial but it also may not exist [63, §5.1].

Kantorovich proposed the relaxation of the Monge's problem and presented the formulation in which a solution always exists [63, §5.1]. The Kantorovich problem aims to find a joint distribution over the \mathbb{P} and the \mathbb{Q} that determines how the mass is allocated. To find an optimal solution, it is necessary to build the cost matrix for all $\mathbf{x} \in X$ and $\mathbf{y} \in Y$ samples:

$$M_{XY} \stackrel{\text{def}}{=} [c(\mathbf{x}_i, \mathbf{y}_j)]_{ij} \quad (2)$$

Having the cost matrix M_{XY} , we are searching for the optimal coupling γ , that minimizes the displacement cost between two probability measures \mathbb{P} and \mathbb{Q}

$$W_p^p(\mathbb{P}, \mathbb{Q}) = \min_{\gamma \in U(a,b)} \langle \gamma, M_{XY} \rangle \quad (3)$$

with the constraints to the coupling $\gamma \in U(a, b)$ such that:

$$U(a, b) \stackrel{\text{def}}{=} \{ \gamma \in \mathbb{R}_+^{n \times m} \mid \gamma \mathbf{1}_m = a, \gamma^\top \mathbf{1}_n = b \} \quad (4)$$

The infimum of this optimization problem induces the Wasserstein distance, and coupling γ gives us a non-bijective map between probability measures \mathbb{P} and \mathbb{Q} .

2.1.1 Cyclical monotonicity

The main geometric property of the OT maps is c -cyclical monotonicity. Formally the map is c -cyclically monotone if for all points $\mathbf{x}_0 \dots \mathbf{x}_i, \mathbf{y}_0 \dots \mathbf{y}_i$ holds:

$$\sum_{i=1}^N c(\mathbf{x}_i, \mathbf{y}_i) \leq \sum_{i=1}^N c(\mathbf{x}_i, \mathbf{y}_{i+1}) \quad (5)$$

A c -cyclically monotone map cannot be improved in terms of the cost function c [63, §5]. It is critical to have this property between two domains in DA because OT solver always **aims to find a c -cyclically monotone map** [63, §5]. If two distribution samples \mathbf{x}_n and \mathbf{y}_n are c -cyclically monotone, and at the same time, their labels are equal for each n , OT can map one distribution to another while preserving a class-wise structure. In practice, when cost c is Euclidean, samples in different domains with the same labels are not always the closest. This leads to the behavior when OT maps samples into the wrong classes.

3 Related Work

Optimal transport for domain adaptation: Optimal transport map labeled source samples in \mathbb{Q} to the unlabeled or partly labeled samples in target \mathbb{P} . Different linear programming solvers can be used to find a solution to the mass transport problem; for example, the Dantzig simplex [39] methods are actively used in various OT solvers like Earth Mover’s Distance (EMD) [7, 14]. For differentiable OT, the Sinkhorn algorithm [9] was proposed. The Sinkhorn is based on the matrix-vector multiplication operations and can be combined with various regularizations like group lasso regularization (L1L2) and Laplacian regularization (L1LP) [7]. To make the OT applicable to the out-of-sample mapping, a linear OT mapping estimator (OTLin) was proposed [45]. OTLin jointly computes the coupling γ (3) and maps T linked to the original Monge problem (1).

The Inverse OT algorithms can reconstruct the cost function that saves the underlying data structure during mapping [28]. Recently it was shown that the cost function could be approximated by the neural network and the given labels [31]. To train the cost function, it is necessary to solve the transport problem using the Sinkhorn algorithm [9] at every optimization step [31]. These methods are hardly scalable and have not been applied to solve DA problems.

The connection between OT and deep networks was proposed for the unsupervised DA [10] and transfer learning [29]. In DA with label and target shift problems, OT methods align probability distributions between a few domains [49, 48].

Deep domain adaptation: Alternately, the task of DA is to make the target domain \mathbb{P} samples closer to the source domain \mathbb{Q} samples. In this setting, the goal is to adapt the source classifier f_θ to the unlabeled target domain samples \mathbb{P} [3, 4, 16]. Usually, a small number of labeled samples are available in the target domain. Standard approaches to this problem are distance-based algorithms [18, 32, 34] or adversarial-based algorithms like DANN [15], CDAN, CDAN-E [33]. These methods show high accuracy but require time-consuming computations. In comparison to the deep DA methods, OT has lower computational complexity and theoretical guarantees in domain adaptation [50]. In our paper **we consider deep DA problem setting** to improve the accuracy of the source classifier f_θ on the target data using simple OT solvers instead of neural networks.

Adversarial attacks: Previously, the various properties of adversarial examples were studied [46, 42, 21]. Applications of adversarial examples for model accuracy improvements were also proposed [65, 68]. The connection between OT and adversarial examples was studied in the context of robustness problems [47, 5]. It has also been shown that the Sinkhorn algorithm could be used to find adversarial perturbations with respect to Wasserstein ball [64]. To the best of our knowledge, we propose the first method that connects the adversarial attacks and optimal transport for domain adaptation.

4 Proposed method

In this section, we present a new algorithm that generates a new domain by the inverse adversarial attack. Before introducing the algorithm, we outline motivation to use an adversarial attack to generate a *source fiction* domain.

4.1 Adversarial attacks are c -cyclically monotone

Adversarial examples are samples that are similar to the true samples but “fool” a classifier and tend to make incorrect predictions [60]. The phenomenon of the vulnerability of machine learning models to adversarial examples raises a great deal of concern in many learning scenarios [43, 69, 57, 66]. With small changes described in 4.2, the adversarial attack can turn any sample into an accurately classified one in the same way that is used to “fool” the classifier. In our paper, we consider the simplest adversarial attack: Fast Sign Gradient Descent (FSGD) [17]. The iterative version of FSGD can be presented as:

$$\mathbf{x}'_0 = \mathbf{x}, \quad \mathbf{x}'_{i+1} = \text{clip}_{\mathbf{x}, \varepsilon} \{ \mathbf{x}'_i - \alpha \text{sign}(\nabla_{\mathbf{x}} L(\theta, \mathbf{x}'_i, \mathbf{y})) \} \quad (6)$$

With sample \mathbf{x} , label \mathbf{y} , and classifier f_θ , we can obtain adversarial examples using gradient descent perturbations, maximizing the loss L on a sample \mathbf{x} with respect to some perturbation size ε . Adversarial attacks with a small parameter ε are c -cyclically monotone maps, i.e., OT. With mild assumptions on adversarial attack we prove that it is a c -cyclically monotone transformation of the data w.r.t. the quadratic cost $c(\mathbf{x}, \mathbf{y}) = \frac{1}{2} \|\mathbf{x} - \mathbf{y}\|^2$.

Lemma 4.1 (cyclical monotonicity of small perturbations of a dataset.). *Let $\mathbf{x}_1, \dots, \mathbf{x}_N \in \mathbb{R}^D$ be a dataset of N distinct samples. Let $\mathbf{x}'_1, \dots, \mathbf{x}'_N$ be its ε -perturbation, i.e. $\|\mathbf{x}_n - \mathbf{x}'_n\| \leq \varepsilon$ for all $n = 1, 2, \dots, N$. Assume that $\varepsilon \leq \frac{1}{2} \min_{n_1, n_2} \|\mathbf{x}_{n_1} - \mathbf{x}_{n_2}\|$, i.e. the perturbation does not exceed $\frac{1}{2}$ of the minimal pairwise distance between samples, then $\leq \varepsilon$ -perturbation is c -cyclically monotone.*

Adversarial attacks are small ε perturbations of the dataset samples, we immediately obtain:

Corollary 4.2. *Let $x_1, \dots, x_N \in \mathbb{R}^D$ be a dataset of N distinct samples. Then any adversarial attack $\mathbf{x}_n \mapsto \mathbf{x}'_n$ on the dataset with $\varepsilon \leq \frac{1}{2} \min_{n_1, n_2} \|\mathbf{x}_{n_1} - \mathbf{x}_{n_2}\|$ is c -cyclically monotone.*

The proof of lemma is in Appendix (§A.1). Corollary 4.2 suggests to use the *optimal* map to transform target domain \mathbb{Q} to domain \mathbb{P}' formed by the c -cyclically monotone *inverse adversarial attack*.

4.2 Domain adaptation with source fiction

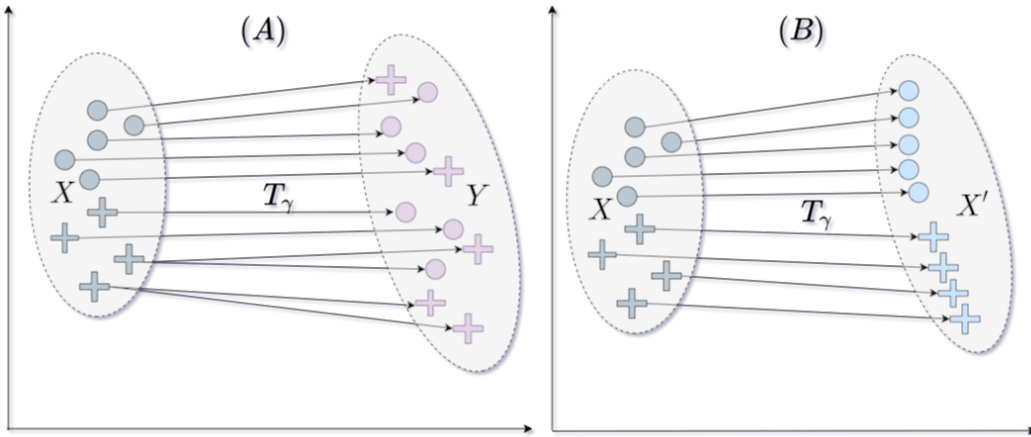


Figure 1: Illustration of the difference between two settings. (A) Optimal transport T_γ between the target X and source Y domain samples. (B) Optimal transport mapping between target and the proposed *source fiction* domain samples X' . The figure illustrates the example with the two classes in each domain (circles and crosses). By the lines, connected the “closest w.r.t the Euclidean distance” samples between the two domains. In (A), the samples from the same class in the two domains are not always closest. In (B), samples in the target domain are the closest to the corresponding class sample in the *source fiction*.

Algorithm 1 Algorithm for DA with *source fiction*

Input: Classifier f_θ , OT algorithm T , source samples Y , labeled X_l and all target samples X , perturbations size ε
Initialize: $\varepsilon \leq \frac{1}{2} \min_{n_1, n_2} \|\mathbf{x}_{n_1} - \mathbf{x}_{n_2}\|$ for \mathbf{x}_n in labeled X_l
Pretrain classifier f_θ on source
 $Y' \leftarrow \emptyset$
for $\mathbf{x}, \mathbf{y} \in X_l$ **do**
 $\mathbf{x}' \leftarrow \mathbf{x}$
 for some iterations **do**
 $\mathbf{x}' \leftarrow \text{clip}_{\mathbf{x}, \varepsilon} \{\mathbf{x}'_n - \alpha \text{sign}(\nabla_x L(\theta, \mathbf{x}', \mathbf{y}))\}$
 end for
 Add \mathbf{x}' to X'
end for
Find a map $X \rightarrow X'$ using T .
Apply the classifier f_θ to the output of T .
return Trained classifier f_θ and map T .

As we proved, adversarial attacks are c -cyclically monotone transformation over the dataset 4.2. To manage this property, we replace the source with the distribution that is cyclically monotone to the target distribution and is, at the same time, accurately classified by a source classifier.

In our method, we use a targeted FSGD adversarial attack (Eq. (6)) to source classifier f_θ , with target label \mathbf{y} equal to the true class of the given sample. Such attack adds to the image features of the class it really belongs to [21]. By inverse adversarial attack we obtain a new distribution \mathbb{P}' with samples $X \subset \mathbb{R}^D$. Following corollary 4.2 to obtain monotonicity, we set the size of perturbation $\varepsilon \leq \frac{1}{2} \min_{n_1, n_2} \|\mathbf{x}_{n_1} - \mathbf{x}_{n_2}\|$ for all \mathbf{x}_n in X_l .

For each labeled sample X_l in the target distribution, we obtain a corresponding samples X' . While X' is a cyclically monotone transformation of the target, we have a low quadratic cost between each target sample X_l and its corresponding sample in X' . To apply adaptation of classifier f_θ on the target distribution samples without labels, we use OT to find a map between all samples from the distribution X and X' . The pipeline of OT for DA with samples X' is presented in Algorithm 4.2.

5 Experiments

In this section, we test our method on two types of datasets (§5.1). The experiments aim to demonstrate that our method improves the performance of fundamental discrete OT algorithms. Besides, we compare different deep DA baselines 5.2. Discussion on empirical complexity is presented in Section (§5.6). Additionally, we conduct an ablation study on the ε parameter to show the stability of our method in different settings of the inverse adversarial attack. The code is written in *PyTorch* framework and will be made public. We give more training details (pre-processing, architectures, etc.) in Appendix (§A.4).

5.1 Datasets

Digits: We evaluated our method on Digits datasets MNIST [26], USPS [20], SVNH [40], and MNIST-M [15]. Each dataset consists of 10 classes of digit images with different numbers of train and test samples. We resized the images to the (32×32) pixel size as a pre-processing step.

Modern Office-31: Besides the Digits dataset that consists of only ten classes in each domain, we tested our method on the Modern Office-31 dataset [52] with 31 classes per domain. The Modern Office-31 dataset is one of the most extensive and diverse datasets for DA. The dataset consists of three domains: Amazon (A), Synthetic (S), and Webcam (W). In comparison to the Digits and original Office-31 dataset [55], this dataset includes synthetic \rightarrow real task, which is problematic. Additionally, we included the DLSR (D) domain from the original Office-31 to estimate our algorithm properly, see the results in Appendix (§A.4).

5.2 Baselines

Deep domain adaptation algorithms: We considered the range of fundamental gradient-based DA techniques. First of all, we compared our method to the prominent adversarial-based approach DANN [15], CDAN, CDAN-E [33]. We also tested the Maximum Mean Discrepancy (MMD) [18] based DA techniques like DAN [32] and JAN [34]. Additionally, we considered the Wasserstein distance-based method WDGRL [58]. We used implementation for this methods proposed in in ADA framework [62]. For the Modern Office-31 experiments we compared our method to the RSDA-DANN [52], SymNet [70], and CAN [22] methods.

Neural optimal transport: Following the benchmark results of the neural OT algorithms benchmark [24], we choose two methods to apply DA: W2GN [23] and MM:R [41, 24]. We used Dense ICNN [23] with three hidden layers [64, 64, 32] as potentials ϕ and ψ in for W2GN and MM:R neural OT methods. Potentials are pertained to apply invariant transformation using Adam [54] optimizer with lr equal to $1e-4$. Methods are trained 300 epochs with Adam optimizer and lr equal to $1e-3$.

Discrete OT solvers: We tested several OT solvers in semi-supervised domain adaptation settings: EMD [7], Sinkhorn [9], SinkhornL1L2, SinkhornLPL2, and OTLin [45]. Most of these algorithms are presented in the POT framework [14], which provides state-of-the-art OT solvers for DA. For experiments, we used quadratic cost $c(\mathbf{x}, \mathbf{y}) = \frac{1}{2}\|\mathbf{x} - \mathbf{y}\|^2$ for each algorithm. Regularization size equals 4.0 for Sinkhorn, SinkhornL1L2, SinkhornLPL2, and OTLin; all other hyperparameters are equal to the default, presented in POT.

5.3 Settings

For the source domain classifier, we trained ResNet50 [19] to achieve 90+ accuracy on the test set of each domain in Digits and Modern Office-31. The classifier was trained using Adam [54] optimizer with a $1e-3$ learning rate. The size of latent space before the output layer was equal to 2048. After training, we applied DA by moving mass in the latent space of the source classifier. For discrete OT baselines, the available labels were used to penalty the transport plan by building a cost matrix M with $M(i, j) = 0$ when \mathbf{x}_i and \mathbf{y}_j labels are equal and $+\infty$ if not [8, 67]

Class	Method	M \rightarrow S	S \rightarrow M	M \rightarrow U	M \rightarrow MM
Deep DA	Source	22.0	79.0	74.1	33.5
	DANN	19.5	61.7	93.8	37.5
	C-DAN	11.5	79.0	90.7	68.4
	CDAN-E	11.3	77.9	90.3	69.6
	DAN	16.7	54.8	95.0	47.0
	JAN	11.5	57.9	89.5	52.9
	WDGRL	13.8	59.5	85.7	52.0
	W2GN	20.4	79.9	89.1	74.1
	MM:R	20.3	80.2	78.0	63.8
Discrete OT	EMD	21.2	68.7	79.2	56.1
	OTLin	21.8	69.9	84.1	62.3
	Sinkhorn	21.8	68.8	82.1	55.7
	SinkhornLpL1	21.8	68.8	84.8	55.7
	SinkhornL1L2	21.8	68.8	84.8	55.7
Discrete OT (Ours)	EMD	23.0	86.3	83.1	62.7
	OTLin	<u>25.5</u>	<u>88.4</u>	<u>89.3</u>	<u>64.5</u>
	Sinkhorn	25.5	86.2	83.8	62.9
	SinkhornLpL1	25.5	86.3	88.3	63.0
	SinkhornL1L2	25.5	86.3	88.3	63.0

Table 1: Accuracy \uparrow of different types of DA algorithms in the latent space of source classifier on Digits datasets. For discrete OT methods semi-supervised settings with 10 labeled samples in class are demonstrated. By **bold** we denote highest accuracy, by underline we denote highest accuracy for an discrete OT algorithms

To create a source fiction, we used 50 steps FSGD with ε equal to 0.45. We found that this value allows to achieve strong perturbations and, at the same time, satisfies the proposed bound on all domains. The results are presented in Tables 1, 2. All values in the tables are averaged over the ten runs with randomly chosen sets of labeled samples in the target domain. The top part of the table

represents deep DA and standard discrete OT algorithm results, the bottom part of the table presents the results of discrete OT with *source fiction*.

5.4 Results

Our method demonstrates improvement for all adaptation tasks. The simplest EMD method is less accurate than other methods, and OTLin accuracy is slightly higher for all domains. The Sinkhorn algorithm with group lasso and Laplacian regularizations did not provide notable improvements over standard Sinkhorn. The results with only three known labels in class are presented in Appendix 3.

Our method advances the OT performance, because OT applications for mass moving assume closeness of target \mathbb{P} and source \mathbb{Q} distributions [27]. While OT maps are c -cyclically monotone, i.e., exhibit a specific structure of the map, thus, transportation $X \rightarrow Y$ via OT maps might not be applied to some problems, see [7, Figure 3] for counter-examples. Moreover, discrete OT techniques are susceptible to regularization terms [7, 11, 44] and require special scaling [37].

Class	Method	A \rightarrow S	S \rightarrow A	A \rightarrow W	W \rightarrow A	S \rightarrow W	W \rightarrow S
Deep DA	Source	44.5	6.2	63.3	70.3	5.5	45.6
	RSDA-DANN	76.1	80.8	91.8	90.5	83.1	70.4
	SymNet	65.9	86.8	91.0	89.2	82.2	56.5
	CAN	79.1	91.2	92.8	90.9	89.7	77.9
Discrete OT	EMD	38.4	9.3	45.2	45.6	13.6	36.7
	OTLin	37.1	11.0	38.7	47.5	6.2	39.6
	Sinkhorn	38.0	10.1	44.7	45.5	13.1	37.2
	SinkhornLpL1	38.1	10.4	45.2	45.3	13.1	37.2
	SinkhornL1L2	38.1	10.4	45.0	45.3	13.1	37.2
Discrete OT(Ours)	EMD	56.8	29.7	64.9	73.9	<u>40.1</u>	60.1
	OTLin	58.5	29.8	<u>65.2</u>	<u>74.4</u>	40.1	<u>63.1</u>
	Sinkhorn	57.0	<u>31.0</u>	<u>65.2</u>	73.9	39.9	<u>60.0</u>
	SinkhornLpL1	57.2	31.0	65.2	74.0	40.1	60.1
	SinkhornL1L2	57.2	31.0	65.2	74.0	40.1	60.1

Table 2: Accuracy \uparrow of domain adaptation in the latent space of ResNet50 model on Modern Office-31 dataset in semi-supervised settings with the 10 known labels for each class in the target domain. By **bold** we denote highest accuracy, by underline we denote highest accuracy for an discrete OT algorithm

The method presented in the paper is efficient, because OT can find a map between a target and a source and, at the same time, save discriminativity, i.e., class-wise structure. In our pipeline, OT maps the unlabeled samples to the perturbed samples from the same class in the *source fiction*. In practice, the distance between samples inside the classes is less than the distance between samples from different classes. The Appendix section (§A.4) presents the adaptation results with only 3 labels per class.

5.5 Ablation study on ε parameter

In this section, we show the adaptation results with different ε values in the FSGD algorithm. We evaluated few transportation tasks: MNIST \rightarrow USPS, USPS \rightarrow MNIST, MNIST \rightarrow MNIST-M, and MNIST \rightarrow SVHN datasets with different values of ε . The value of $\frac{1}{2} \min_{n_1, n_2} \|x_{n_1} - x_{n_2}\|$ is different for various datasets, for SVHN this value is 0.74, for MNIST is 0.29, for MNIST-M is 10.9 and for USPS is equal to 0.85. We compute these values in the latent space of the ResNet50 classifier trained on the corresponding domain. For each domain, we use different values of ε and then fit OT to find a map between target and *source fiction*. Our results show a small trade-off between the size of perturbations and the cyclical monotonicity. Figure 2 illustrates the adaptation accuracy with different ε .

When the ε value becomes larger than $\frac{1}{2}$ min distance between samples, the accuracy of adaptation decreases because the transformation becomes less c -cyclically monotone. With a small value of ε , the adaptation achieves the highest accuracy. With larger perturbations, the prediction of the classifier on perturbed samples becomes more accurate (see FSGD curve in Figure 2) until perturbation size

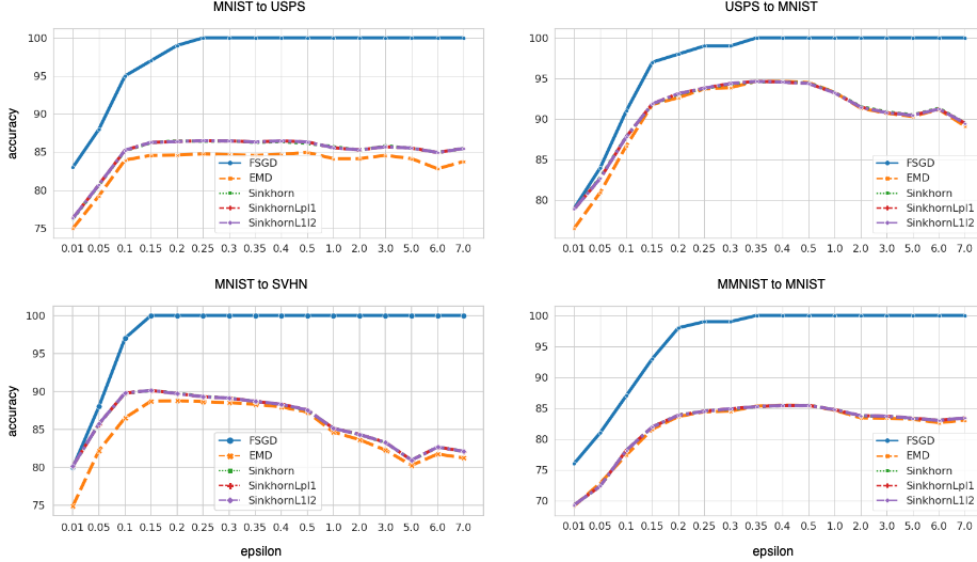


Figure 2: Results of ablation on ε parameter for MNIST \rightarrow MNIST-M (left) and SVHN \rightarrow MNIST (right) datasets. FSGD denotes how accurately the source domain model classifies *source fiction* samples obtained with the corresponding parameter ε .

achieves the ε bound. With perturbations a little bit larger than the ε bound, most of the samples in *source fiction* are still c -cyclically monotone to the target and the method still works.

5.6 Empirical complexity

The method proposed improves discrete OT methods in domain adaptation. This is an important achievement, because discrete OT methods are a very simple and fast technique for DA compared to the approaches based on deep neural networks. Deep domain adaptation methods are complex, typically solve the challenging min-max optimization, and take hours of training.

In practice, depending on the dataset size and source domain classifier architecture, discrete OT methods like EMD, Sinkhorn, and OTLin take 10-30 minutes to solve domain adaptation on GPU GeForce GTX-1080 (12 GB). As we created the *source fiction* based only on a small number of labeled target samples, an inverse adversarial attack takes less than a minute.

6 Discussion

Potential impact: The important property of discrete transport methods is their ability to be quickly applied to the new adaptation tasks. Usually, in DA, it is necessary to modify classifier architecture and train separately on each target domain [15, 33, 32, 34, 18]. OT solves domain adaptation by moving target domain samples closer to the source data, and it is unnecessary to change or fine-tune the source classifier. In this paper, we presented an algorithm that improves OT performance. Using OT, a single source domain classifier can make predictions on a range of target domains without any modification.

Nowadays, the data is shared on separate devices and usually contains personal information, which is inefficient for data transmission and may violate data privacy. The authors of the [30] addresses a challenging DA setting without access to the source data for higher privacy. In our method, we adapt the source classifier to the new domain without access to the source data, using only source classifier, which can be used in various scenarios to avoid privacy issues.

Limitations: The main limitation of our approach is that it is necessary to have access to the labels in the target domain. To avoid the limitation of labels availability, we plan to use pseudo-labeling techniques.

7 Conclusion

We proposed an algorithm that modifies DA toward making target data closer to the domain formed by an adversarial attack and proved that adversarial attacks are OT maps over the datasets. We conducted various experiments on different datasets and showed that our method improves OT baselines. In some domains for discrete OT methods, adaptation with *source fiction* improved accuracy by more than 10 percent.

Our method provides many straightforward applications. Neural OT is applied in the modern generative modeling approach. We plan to adapt our approach to neural transport solvers to make the method robust to out-of-sample estimation. While OT can solve DA with target shift and unbalanced classes [49, 48], it is promising to use *source fiction* for such problems. Pseudo-labeling techniques to turn the method into a fully unsupervised method is also a promising direction. We expect our research to contribute to the development of less complicated DA techniques and open doors for the future application of c -cyclical monotonicity of adversarial attacks.

Acknowledgements. This work was supported by the Analytical Center for the Government of the Russian Federation (IGK 000000D730321P5Q0002), agreement No. 70-2021-00141.

References

- [1] Brandon Amos, Lei Xu, and J. Zico Kolter. Input convex neural networks. In Doina Precup and Yee Whye Teh, editors, *Proceedings of the 34th International Conference on Machine Learning, ICML 2017, Sydney, NSW, Australia, 6-11 August 2017*, volume 70 of *Proceedings of Machine Learning Research*, pages 146–155. PMLR, 2017.
- [2] Martin Arjovsky, Soumith Chintala, and Léon Bottou. Wasserstein generative adversarial networks. In *International conference on machine learning*, pages 214–223. PMLR, 2017.
- [3] Shai Ben-David, John Blitzer, Koby Crammer, Alex Kulesza, Fernando Pereira, and Jennifer Wortman Vaughan. A theory of learning from different domains. *Mach. Learn.*, 79(1-2):151–175, 2010.
- [4] Shai Ben-David, Tyler Lu, Teresa Luu, and Dávid Pál. Impossibility theorems for domain adaptation. In Yee Whye Teh and D. Mike Titterton, editors, *Proceedings of the Thirteenth International Conference on Artificial Intelligence and Statistics, AISTATS 2010, Chia Laguna Resort, Sardinia, Italy, May 13-15, 2010*, volume 9 of *JMLR Proceedings*, pages 129–136. JMLR.org, 2010.
- [5] Quentin Bouniot, Romaric Audigier, and Angelique Loesch. Optimal transport as a defense against adversarial attacks. In *2020 25th International Conference on Pattern Recognition (ICPR)*, pages 5044–5051. IEEE, 2021.
- [6] Pierre Colombo, Guillaume Staerman, Chloe Clavel, and Pablo Piantanida. Automatic text evaluation through the lens of wasserstein barycenters. *arXiv preprint arXiv:2108.12463*, 2021.
- [7] Nicolas Courty, Rémi Flamary, Devis Tuia, and Alain Rakotomamonjy. Optimal transport for domain adaptation. *CoRR*, abs/1507.00504, 2015.
- [8] Nicolas Courty, Rémi Flamary, Devis Tuia, and Alain Rakotomamonjy. Optimal transport for domain adaptation. *IEEE transactions on pattern analysis and machine intelligence*, 39(9):1853–1865, 2016.
- [9] Marco Cuturi. Sinkhorn distances: Lightspeed computation of optimal transport. In Christopher J. C. Burges, Léon Bottou, Zoubin Ghahramani, and Kilian Q. Weinberger, editors, *Advances in Neural Information Processing Systems 26: 27th Annual Conference on Neural Information Processing Systems 2013. Proceedings of a meeting held December 5-8, 2013, Lake Tahoe, Nevada, United States*, pages 2292–2300, 2013.
- [10] Bharath Bhushan Damodaran, Benjamin Kellenberger, Rémi Flamary, Devis Tuia, and Nicolas Courty. Deepjdot: Deep joint distribution optimal transport for unsupervised domain adaptation. In *Proceedings of the European Conference on Computer Vision (ECCV)*, pages 447–463, 2018.
- [11] Arnaud Dessein, Nicolas Papadakis, and Jean-Luc Rouas. Regularized optimal transport and the rot mover’s distance. *The Journal of Machine Learning Research*, 19(1):590–642, 2018.

- [12] Jiaojiao Fan, Amirhossein Taghvaei, and Yongxin Chen. Scalable computations of wasserstein barycenter via input convex neural networks. *CoRR*, abs/2007.04462, 2020.
- [13] Sira Ferradans, Nicolas Papadakis, Gabriel Peyré, and Jean-François Aujol. Regularized discrete optimal transport. *SIAM Journal on Imaging Sciences*, 7(3):1853–1882, 2014.
- [14] Rémi Flamary, Nicolas Courty, Alexandre Gramfort, Mokhtar Zahdi Alaya, Aurélie Boisbunon, Stanislas Chambon, Laetitia Chapel, Adrien Corenflos, Kilian Fatras, Nemo Fournier, et al. Pot: Python optimal transport. *Journal of Machine Learning Research*, 22(78):1–8, 2021.
- [15] Yaroslav Ganin and Victor S. Lempitsky. Unsupervised domain adaptation by backpropagation. In Francis R. Bach and David M. Blei, editors, *Proceedings of the 32nd International Conference on Machine Learning, ICML 2015, Lille, France, 6-11 July 2015*, volume 37 of *JMLR Workshop and Conference Proceedings*, pages 1180–1189. JMLR.org, 2015.
- [16] Pascal Germain, Amaury Habrard, François Laviolette, and Emilie Morvant. A pac-bayesian approach for domain adaptation with specialization to linear classifiers. In *Proceedings of the 30th International Conference on Machine Learning, ICML 2013, Atlanta, GA, USA, 16-21 June 2013*, volume 28 of *JMLR Workshop and Conference Proceedings*, pages 738–746. JMLR.org, 2013.
- [17] Ian J Goodfellow, Jonathon Shlens, and Christian Szegedy. Explaining and harnessing adversarial examples. *arXiv preprint arXiv:1412.6572*, 2014.
- [18] Arthur Gretton, Karsten M. Borgwardt, Malte J. Rasch, Bernhard Schölkopf, and Alexander J. Smola. A kernel two-sample test. *J. Mach. Learn. Res.*, 13:723–773, 2012.
- [19] Kaiming He, Xiangyu Zhang, Shaoqing Ren, and Jian Sun. Deep residual learning for image recognition. In *Proceedings of the IEEE conference on computer vision and pattern recognition*, pages 770–778, 2016.
- [20] J. J. Hull. A database for handwritten text recognition research. *IEEE Transactions on Pattern Analysis and Machine Intelligence*, 16(5):550–554, 1994.
- [21] Andrew Ilyas, Shibani Santurkar, Dimitris Tsipras, Logan Engstrom, Brandon Tran, and Aleksander Madry. Adversarial examples are not bugs, they are features. *CoRR*, abs/1905.02175, 2019.
- [22] Guoliang Kang, Lu Jiang, Yi Yang, and Alexander G Hauptmann. Contrastive adaptation network for unsupervised domain adaptation. In *Proceedings of the IEEE/CVF Conference on Computer Vision and Pattern Recognition*, pages 4893–4902, 2019.
- [23] Alexander Korotin, Vage Egiazarian, Arip Asadulaev, and Evgeny Burnaev. Wasserstein-2 generative networks. *CoRR*, abs/1909.13082, 2019.
- [24] Alexander Korotin, Lingxiao Li, Aude Genevay, Justin Solomon, Alexander Filippov, and Evgeny Burnaev. Do neural optimal transport solvers work? a continuous wasserstein-2 benchmark. *arXiv preprint arXiv:2106.01954*, 2021.
- [25] Alexander Korotin, Lingxiao Li, Justin Solomon, and Evgeny Burnaev. Continuous wasserstein-2 barycenter estimation without minimax optimization. *CoRR*, abs/2102.01752, 2021.
- [26] Yann LeCun and Corinna Cortes. MNIST handwritten digit database. 2010.
- [27] John Lee, Max Dabagia, Eva L Dyer, and Christopher J Rozell. Hierarchical optimal transport for multimodal distribution alignment. *arXiv preprint arXiv:1906.11768*, 2019.
- [28] Ruilin Li, Xiaojing Ye, Haomin Zhou, and Hongyuan Zha. Learning to match via inverse optimal transport. *Journal of machine learning research*, 20, 2019.
- [29] Xuhong Li, Yves Grandvalet, Rémi Flamary, Nicolas Courty, and Dejing Dou. Representation transfer by optimal transport. *arXiv preprint arXiv:2007.06737*, 2020.
- [30] Jian Liang, Dapeng Hu, and Jiashi Feng. Do we really need to access the source data? source hypothesis transfer for unsupervised domain adaptation. In *Proceedings of the 37th International Conference on Machine Learning, ICML 2020, 13-18 July 2020, Virtual Event*, volume 119 of *Proceedings of Machine Learning Research*, pages 6028–6039. PMLR, 2020.
- [31] Ruishan Liu, Akshay Balsubramani, and James Zou. Learning transport cost from subset correspondence. *arXiv preprint arXiv:1909.13203*, 2019.

- [32] Mingsheng Long, Yue Cao, Jianmin Wang, and Michael I. Jordan. Learning transferable features with deep adaptation networks. In Francis R. Bach and David M. Blei, editors, *Proceedings of the 32nd International Conference on Machine Learning, ICML 2015, Lille, France, 6-11 July 2015*, volume 37 of *JMLR Workshop and Conference Proceedings*, pages 97–105. JMLR.org, 2015.
- [33] Mingsheng Long, Zhangjie Cao, Jianmin Wang, and Michael I. Jordan. Conditional adversarial domain adaptation. In Samy Bengio, Hanna M. Wallach, Hugo Larochelle, Kristen Grauman, Nicolò Cesa-Bianchi, and Roman Garnett, editors, *Advances in Neural Information Processing Systems 31: Annual Conference on Neural Information Processing Systems 2018, NeurIPS 2018, December 3-8, 2018, Montréal, Canada*, pages 1647–1657, 2018.
- [34] Mingsheng Long, Han Zhu, Jianmin Wang, and Michael I. Jordan. Deep transfer learning with joint adaptation networks. In Doina Precup and Yee Whye Teh, editors, *Proceedings of the 34th International Conference on Machine Learning, ICML 2017, Sydney, NSW, Australia, 6-11 August 2017*, volume 70 of *Proceedings of Machine Learning Research*, pages 2208–2217. PMLR, 2017.
- [35] Ashok Vardhan Makkuva, Amirhossein Taghvaei, Sewoong Oh, and Jason D. Lee. Optimal transport mapping via input convex neural networks. In *Proceedings of the 37th International Conference on Machine Learning, ICML 2020, 13-18 July 2020, Virtual Event*, volume 119 of *Proceedings of Machine Learning Research*, pages 6672–6681. PMLR, 2020.
- [36] Robert J McCann. Existence and uniqueness of monotone measure-preserving maps. *Duke Mathematical Journal*, 80(2):309–323, 1995.
- [37] Cheng Meng, Yuan Ke, Jingyi Zhang, Mengrui Zhang, Wenxuan Zhong, and Ping Ma. Large-scale optimal transport map estimation using projection pursuit. *arXiv preprint arXiv:2106.05838*, 2021.
- [38] Youssef Mroueh. Wasserstein style transfer. *arXiv preprint arXiv:1905.12828*, 2019.
- [39] John C Nash. The (dantzig) simplex method for linear programming. *Computing in Science & Engineering*, 2(1):29–31, 2000.
- [40] Yuval Netzer, Tao Wang, Adam Coates, Alessandro Bissacco, Bo Wu, and Andrew Y Ng. Reading digits in natural images with unsupervised feature learning. 2011.
- [41] Quan Hoang Nhan Dam, Trung Le, Tu Dinh Nguyen, Hung Bui, and Dinh Phung. Threeplayer wasserstein gan via amortised duality. In *Proc. of the 28th Int. Joint Conf. on Artificial Intelligence (IJCAI)*, 2019.
- [42] Nicolas Papernot, Patrick D. McDaniel, and Ian J. Goodfellow. Transferability in machine learning: from phenomena to black-box attacks using adversarial samples. *CoRR*, abs/1605.07277, 2016.
- [43] Nicolas Papernot, Patrick D. McDaniel, Ian J. Goodfellow, Somesh Jha, Z. Berkay Celik, and Ananthram Swami. Practical black-box attacks against machine learning. In *Proceedings of the 2017 ACM on Asia Conference on Computer and Communications Security, AsiaCCS 2017, Abu Dhabi, United Arab Emirates, April 2-6, 2017*, pages 506–519, 2017.
- [44] François-Pierre Paty and Marco Cuturi. Regularized optimal transport is ground cost adversarial. In *International Conference on Machine Learning*, pages 7532–7542. PMLR, 2020.
- [45] Michaël Perrot, Nicolas Courty, Rémi Flamary, and Amaury Habrard. Mapping estimation for discrete optimal transport. In Daniel D. Lee, Masashi Sugiyama, Ulrike von Luxburg, Isabelle Guyon, and Roman Garnett, editors, *Advances in Neural Information Processing Systems 29: Annual Conference on Neural Information Processing Systems 2016, December 5-10, 2016, Barcelona, Spain*, pages 4197–4205, 2016.
- [46] Deyan Petrov and Timothy M. Hospedales. Measuring the transferability of adversarial examples. *CoRR*, abs/1907.06291, 2019.
- [47] Muni Sreenivas Pydi and Varun Jog. Adversarial risk via optimal transport and optimal couplings. In *International Conference on Machine Learning*, pages 7814–7823. PMLR, 2020.
- [48] Alain Rakotomamonjy, Rémi Flamary, Gilles Gasso, Mokhtar Z Alaya, Maxime Berar, and Nicolas Courty. Optimal transport for conditional domain matching and label shift. *arXiv preprint arXiv:2006.08161*, 2020.

- [49] Ievgen Redko, Nicolas Courty, Rémi Flamary, and Devis Tuia. Optimal transport for multi-source domain adaptation under target shift. In *The 22nd International Conference on Artificial Intelligence and Statistics*, pages 849–858. PMLR, 2019.
- [50] Ievgen Redko, Amaury Habrard, and Marc Sebban. Theoretical analysis of domain adaptation with optimal transport. In *Joint European Conference on Machine Learning and Knowledge Discovery in Databases*, pages 737–753. Springer, 2017.
- [51] Sebastian Reich. A nonparametric ensemble transform method for bayesian inference. *SIAM Journal on Scientific Computing*, 35(4):A2013–A2024, 2013.
- [52] Tobias Ringwald and Rainer Stiefelhagen. Adaptiope: A modern benchmark for unsupervised domain adaptation. In *Proceedings of the IEEE/CVF Winter Conference on Applications of Computer Vision*, pages 101–110, 2021.
- [53] Ralph Rockafellar. Characterization of the subdifferentials of convex functions. *Pacific Journal of Mathematics*, 17(3):497–510, 1966.
- [54] Sebastian Ruder. An overview of gradient descent optimization algorithms. *CoRR*, abs/1609.04747, 2016.
- [55] Kate Saenko, Brian Kulis, Mario Fritz, and Trevor Darrell. Adapting visual category models to new domains. In *European conference on computer vision*, pages 213–226. Springer, 2010.
- [56] Filippo Santambrogio. Optimal transport for applied mathematicians. calculus of variations, pdes and modeling. 2015.
- [57] Lukas Schott, Jonas Rauber, Matthias Bethge, and Wieland Brendel. Towards the first adversarially robust neural network model on MNIST. In *7th International Conference on Learning Representations, ICLR 2019, New Orleans, LA, USA, May 6-9, 2019*, 2019.
- [58] Jian Shen, Yanru Qu, Weinan Zhang, and Yong Yu. Wasserstein distance guided representation learning for domain adaptation. In *Thirty-second AAAI conference on artificial intelligence*, 2018.
- [59] Justin Solomon, Fernando De Goes, Gabriel Peyré, Marco Cuturi, Adrian Butscher, Andy Nguyen, Tao Du, and Leonidas Guibas. Convolutional wasserstein distances: Efficient optimal transportation on geometric domains. *ACM Transactions on Graphics (TOG)*, 34(4):1–11, 2015.
- [60] Christian Szegedy, Wojciech Zaremba, Ilya Sutskever, Joan Bruna, Dumitru Erhan, Ian J. Goodfellow, and Rob Fergus. Intriguing properties of neural networks. In Yoshua Bengio and Yann LeCun, editors, *2nd International Conference on Learning Representations, ICLR 2014, Banff, AB, Canada, April 14-16, 2014, Conference Track Proceedings*, 2014.
- [61] Amirhossein Taghvaei and Amin Jalali. 2-wasserstein approximation via restricted convex potentials with application to improved training for gans. *CoRR*, abs/1902.07197, 2019.
- [62] Anne-Marie Tousch and Christophe Renaudin. (yet) another domain adaptation library, 2020.
- [63] C. Villani. *Optimal Transport: Old and New*. Grundlehren der mathematischen Wissenschaften. Springer Berlin Heidelberg, 2008.
- [64] Eric Wong, Frank R. Schmidt, and J. Zico Kolter. Wasserstein adversarial examples via projected sinkhorn iterations. In *Proceedings of the 36th International Conference on Machine Learning, ICML 2019, 9-15 June 2019, Long Beach, California, USA*, pages 6808–6817, 2019.
- [65] Cihang Xie, Mingxing Tan, Boqing Gong, Jiang Wang, Alan L. Yuille, and Quoc V. Le. Adversarial examples improve image recognition. *CoRR*, abs/1911.09665, 2019.
- [66] Cihang Xie, Jianyu Wang, Zhishuai Zhang, Yuyin Zhou, Lingxi Xie, and Alan Yuille. Adversarial examples for semantic segmentation and object detection. In *Proceedings of the IEEE International Conference on Computer Vision*, pages 1369–1378, 2017.
- [67] Yuguang Yan, Wen Li, Hanrui Wu, Huaqing Min, Mingkui Tan, and Qingyao Wu. Semi-supervised optimal transport for heterogeneous domain adaptation. In *IJCAI*, volume 7, pages 2969–2975, 2018.
- [68] Jihan Yang, Ruijia Xu, Ruiyu Li, Xiaojuan Qi, Xiaoyong Shen, Guanbin Li, and Liang Lin. An adversarial perturbation oriented domain adaptation approach for semantic segmentation. In *The Thirty-Fourth AAAI Conference on Artificial Intelligence, AAAI 2020, The Thirty-Second Innovative Applications of Artificial Intelligence Conference, IAAI 2020, The Tenth AAAI*

Symposium on Educational Advances in Artificial Intelligence, EAAI 2020, New York, NY, USA, February 7-12, 2020, pages 12613–12620. AAAI Press, 2020.

- [69] Xiaoyong Yuan, Pan He, Qile Zhu, and Xiaolin Li. Adversarial examples: Attacks and defenses for deep learning. *IEEE Trans. Neural Netw. Learning Syst.*, 30(9):2805–2824, 2019.
- [70] Yabin Zhang, Hui Tang, Kui Jia, and Minghui Tan. Domain-symmetric networks for adversarial domain adaptation. In *Proceedings of the IEEE/CVF Conference on Computer Vision and Pattern Recognition*, pages 5031–5040, 2019.

A Appendix

A.1 Additional background on OT

OT aims at finding a solution to transfer mass from one distribution to another with the least effort. Monge’s problem was the first example of the OT problem and can be formally expressed as follows:

$$\inf_{T \# \mathbb{P} = \mathbb{Q}} \int_{\Omega_{\mathbb{P}}} c(\mathbf{x}, T(\mathbf{x})) \mathbb{P}(\mathbf{x}) d\mathbf{x} \quad (7)$$

The Monge’s formulation of OT aims at finding a mapping $T : \Omega_{\mathbb{P}} \rightarrow \Omega_{\mathbb{Q}}$ of the two probability measures \mathbb{P} and \mathbb{Q} and a cost function $c : \Omega_{\mathbb{P}} \times \Omega_{\mathbb{Q}} \rightarrow \mathbb{R}_+$, where $T \# \mathbb{P}_s = \mathbb{Q}_t$ represents the mass preserving push forward operator. In Monge’s formulation, T cannot split the mass from a single point. The problem is that the mapping T may not even exist with such constraints.

To avoid this, Kantorovitch proposed a relaxation [63]. Instead of obtaining a mapping, the goal is to seek a joint distribution over the source and the target that determines how the mass is allocated. For a given cost function $c : \Omega_{\mathbb{P}} \times \Omega_{\mathbb{Q}} \rightarrow \mathbb{R}_+$, the primal Kantorovitch formulation can be expressed as the following problem:

$$\min_{\gamma \in \gamma(\mathbb{P}, \mathbb{Q})} \left\{ \int_{\Omega_{\mathbb{P}} \times \Omega_{\mathbb{Q}}} c(\mathbf{x}, \mathbf{y}) d\gamma(\mathbf{x}, \mathbf{y}) = \mathbb{E}_{(\mathbf{x}, \mathbf{y}) \sim \gamma} [c(\mathbf{x}, \mathbf{y})] \right\} \quad (8)$$

In primal Kantorovitch formulation, we look for a joint distribution γ with \mathbb{P} and \mathbb{P} as marginals that minimize the expected transportation cost. If the independent distribution $\gamma(\mathbf{x}, \mathbf{y}) = \mathbb{P}(\mathbf{x})\mathbb{Q}(\mathbf{y})$ respects the constraints, linear program is convex and always has a solution for a semi-continuous c :

$$\gamma(\mathbb{P}, \mathbb{Q}) = \left\{ \gamma \in P(\Omega_{\mathbb{P}}, \Omega_{\mathbb{Q}}) : \int \gamma(\mathbf{x}, \mathbf{y}) d\mathbf{y} = \mathbb{P}(\mathbf{x}), \int \gamma(\mathbf{x}, \mathbf{y}) d\mathbf{x} = \mathbb{Q}(\mathbf{y}) \right\} \quad (9)$$

The primal Kantorovitch formulation can also be presented in dual form as stated by the Rockafellar—Fenchel theorem [63]:

$$\max_{\phi \in C(\Omega_{\mathbb{P}}), \psi \in C(\Omega_{\mathbb{Q}})} \left\{ \int \phi d\mathbb{P} + \int \psi d\mathbb{Q} \mid \phi(\mathbf{x}) + \psi(\mathbf{y}) \leq c(\mathbf{x}, \mathbf{y}) \right\} \quad (10)$$

After finding a solution to the transport problem, OT measures dissimilarity between the two distributions. This similarity is also called the Wasserstein distance [63]:

$$W_p(\mathbb{P}, \mathbb{Q}) = \min_{\gamma \in \gamma(\mathbb{P}, \mathbb{Q})} \left\{ \int_{\Omega_{\mathbb{P}} \times \Omega_{\mathbb{Q}}} c(\mathbf{x}, \mathbf{y}) d\gamma(\mathbf{x}, \mathbf{y}) \right\}^{\frac{1}{p}} \quad (11)$$

where $c(\mathbf{x}, \mathbf{y}) = \|\mathbf{x} - \mathbf{y}\|^p$ and $p > 1$. The Wasserstein distance encodes the geometry of the space through the optimization problem and can be used on any distribution of mass.

A.2 Neural Optimal Transport

Recently, there has been a solid push to incorporate Input Convex Neural Networks (ICNNs) [1] in OT problems. According to Rockafellar’s Theorem [53], every cyclically monotone mapping g is contained in a sub-gradient of some convex function $f : X \rightarrow \mathbb{R}$. Furthermore, according to Brenier’s Theorem (Theorem 1.22 of [56]), these gradients uniquely solve the Monge problem (1). Following these theorems, a range of approaches explored ICNNs as parameterized convex potentials in dual Kantorovitch problem [61, 35].

Further development of this approach enabled the construction of the non-minimax Wasserstein-2 generative framework [23] that can solve DA and Wasserstein-2 Barycenters estimation [12, 25]. Compared to discrete OT, neural methods provide generalized OT methods that can ensure out-of-sample estimates.

A.3 Cyclical monotonicity bound

Lemma A.1 (cyclical monotonicity of small perturbations of a dataset.). *Let $x_1, \dots, x_N \in \mathbb{R}^D$ be a dataset of N distinct samples. Let x'_1, \dots, x'_N be its $\leq \varepsilon$ -perturbation, i.e. $\|x_n - x'_n\| \leq \varepsilon$ for all $n = 1, 2, \dots, N$. Assume that $\varepsilon \leq \frac{1}{2} \min_{n_1, n_2} \|x_{n_1} - x_{n_2}\|$, i.e. the perturbation does not exceed $\frac{1}{2}$ of the minimal pairwise distance between samples. Then for all K and $\overline{1, N}$ it holds:*

$$\sum_{k=1}^K \frac{1}{2} \|x_{n_k} - x'_{n_k}\|^2 \leq \sum_{k=1}^K \frac{1}{2} \|x_{n_k} - x'_{n_{k+1}}\|^2 \quad (12)$$

i.e. set $(x_1, x'_1), \dots, (x_N, x'_N)$ or, equivalently, the map $x_k \mapsto x_{k'}$ is cyclically monotone.

Proof. Due to triangle inequality for $\|\cdot\|$, we have

$$\|x_{n_k} - x'_{n_{k+1}}\| \geq \underbrace{\|x_{n_k} - x_{n_{k+1}}\|}_{\geq 2\varepsilon} - \underbrace{\|x_{n_{k+1}} - x'_{n_{k+1}}\|}_{\leq \varepsilon} = \varepsilon. \quad (13)$$

Taking the square of both sides and summing (13) for $k = 1, 2, \dots, K$ yields

$$\sum_{k=1}^K \|x_{n_k} - x'_{n_{k+1}}\|^2 \geq \sum_{k=1}^K \varepsilon^2 = K\varepsilon^2. \quad (14)$$

Due to the assumptions of the lemma, the following inequality holds true:

$$\sum_{k=1}^K \|x_{n_k} - x'_{n_k}\|^2 \leq \sum_{k=1}^K \varepsilon^2 \leq K\varepsilon^2. \quad (15)$$

We combine (14) and (15) to obtain

$$\sum_{k=1}^K \|x_{n_k} - x'_{n_k}\|^2 \leq \sum_{k=1}^K \|x_{n_k} - x'_{n_{k+1}}\|^2,$$

which is equivalent to

$$\sum_{k=1}^K c(x_{n_k}, x'_{n_k}) \leq \sum_{k=1}^K c(x_{n_k}, x'_{n_{k+1}}), \quad (16)$$

and yield c -cyclically monotone w.r.t. quadratic cost $c(x, y) = \frac{1}{2}\|x - y\|^2$. \square

A.4 Experiments and Details

Pre-processing: We used standard pre-processing over samples with the dataset mean and std normalization. We resize images to 224 x 224 to train the source classifier. No augmentation was used.

Source classifier architectures: For experiments presented in the main section, we used standard ResNet50 [19] from *torchvision* framework. We changed the output layer size to be equal to the number of classes in target and source domains. We trained source classifier to achieve 90+ accuracy on the test set of each domain in Digits and Modern Office-31. The classifier was trained using Adam [54] optimizer with a $1e - 3$ learning rate. The size of latent space before the output layer was equal to 2048. After training, we applied DA by moving mass in the latent space of the source classifier. The same parameters was used to train the ResNet18 source classifier, this results presented in the next subsection.

Additional experiments: In this section, we provide additional experiments using the *source fiction* domain for discrete OT solvers. In tables, **bold** denotes the results of discrete solvers with *source fiction* if this improves its accuracy compared to the standard settings.

Digits dataset results with 3 (Table 3) known labels per class in target domain using ResNet50 classifier.

METHOD	MNIST SVHN	SVHN MNIST	MNIST USPS	USPS MNIST	MNIST M-MNIST
SOURCE	22.0	79.0	63.0	80.0	60.0
EMD	21.3	72.5	66.1	67.8	44.5
SINKHORN	21.7	73.0	67.3	68.7	44.6
SINKHORNLP1	21.7	73.4	67.3	68.8	45.0
SINKHORN1L2	21.7	73.4	67.3	68.8	45.0
OTLIN	21.8	73.4	67.4	68.8	45.0
EMD	23.1	83.5	82.6	86.5	54.7
SINKHORN	23.7	85.0	82.6	86.8	54.8
SINKHORNLP1	23.7	85.2	86.3	86.9	54.9
SINKHORN1L2	23.8	85.2	86.3	86.9	54.9
OTLIN	23.9	85.3	86.3	86.9	55.1

Table 3: Accuracy of domain adaptation by optimal transport in the latent space of ResNet50 model with only 3 known labels for each class in the target domain on Digits datasets. The top part of the table represents semi-supervised settings for discrete OT methods, settings the bottom part presents results using *source fiction*.

Modern-Office dataset results with additional domain DLSR (D) (Table 4), with 10 known labels.

Method	A D	D A	A S	S A	A W	W A	D S	S D	D W	W D	S W	W S
EMD	50.7	46.2	38.4	9.3	45.2	45.6	32.7	16.4	62.6	67.1	13.6	36.7
OTLin	45.8	48.0	37.1	11.0	38.7	47.5	36.5	4.1	60.9	61.8	6.2	39.6
Sinkhorn	51.1	46.3	38.0	10.1	44.7	45.5	32.9	16.5	63.5	67.1	13.1	37.2
SinkhornLpL1	51.1	46.7	38.1	10.4	45.2	45.3	33.0	16.5	63.8	68.3	13.1	37.2
SinkhornL1L2	51.1	46.7	38.1	10.4	45.0	45.3	33.0	16.5	63.8	68.3	13.1	37.2
EMD	70.9	72.5	56.8	29.7	64.9	73.9	56.6	47.3	75.7	75.1	40.1	60.1
OTLin	71.3	73.6	58.5	29.8	65.2	74.4	59.8	47.3	76.6	75.1	40.1	63.1
Sinkhorn	70.6	72.7	57.0	31.0	65.2	73.9	56.7	47.3	77.4	74.8	39.9	60.0
SinkhornLpL1	70.6	72.8	57.2	31.0	65.2	74.0	56.8	47.3	77.4	75.5	40.1	60.1
SinkhornL1L2	70.6	72.8	57.2	31.0	65.2	74.0	56.8	47.3	77.4	75.5	40.1	60.1

Table 4: Results of DA in the latent space of ResNet50 model on Modern Office-31 dataset in semi-supervised settings with the the additional DLSA(D) domain. labels are 10 known for each class in the target domain.

Digits(Table 5) and Modern-Office 6 datasets results using ResNet18 source classifier. 10 labels are known.

METHOD	MNIST SVHN	SVHN MNIST	MNIST USPS	USPS MNIST	MNIST M-MNIST
SOURCE	22.0	79.0	63.0	80.0	60.0
EMD	15.4	64.3	77.0	80.8	70.8
SINKHORN	16.0	65.2	77.9	81.2	70.9
SINKHORN L1LP	16.8	65.7	79.8	85.1	71.8
SINKHORN L1L2	16.0	65.7	79.8	85.1	71.8
OTLIN	16.1	67.1	79.8	86.2	71.8
EMD	35.1	87.1	85.2	95.2	82.3
SINKHORN	38.0	88.3	88.3	95.2	83.5
SINKHORN L1LP	37.1	88.3	88.2	95.2	83.5
SINKHORN L1L2	37.1	88.3	88.3	95.2	83.5
OTLIN	38.0	90.0	88.2	95.2	83.5

Table 5: Accuracy of domain adaptation by optimal transport in the latent space of ResNet18 model with the 10 known labels for each class in the target domain on Digits datasets. The top part of the table represents semi-supervised settings for discrete OT methods, the bottom part presents results using *source fiction*.

METHOD	A D	D A	A S	S A	A W	W A	D S	S D	D W	S W	W S
SOURCE	37	43	25	8	57	41	20	2	65	3	27
EMD	57	42	27	16	53	38	32	28	53	19	37
SINKHORN	58	43	27	17	53	40	32	29	54	20	38
SINKHORN LPL1	58	43	27	17	53	40	32	29	53	20	38
SINKHORN L1L2	58	43	27	17	53	40	32	29	53	20	38
OTLIN	58	43	27	17	53	40	32	29	53	20	38
EMD	76	67	51	44	73	63	59	60	76	45	61
SINKHORN	77	67	51	43	75	63	59	57	77	41	60
SINKHORN LPL1	77	67	51	43	75	63	59	57	77	41	60
SINKHORN L1L2	77	67	51	43	75	63	59	57	77	41	60
OTLIN	77	67	51	43	75	63	59	57	77	41	60

Table 6: Results of domain adaptation in the latent space of ResNet18 model on Modern Office-31 dataset in semi-supervised settings with the 10 known labels for each class in the target domain

CIFAR10-STL10 adaptation task results (Table 7) with ResNet18 source classifier.

METHOD	SOURCE	EMD	SINKH	SINKH L1LP	SINKH L1L2	OTLIN
CIFAR→STL	37.0	48.1	48.1	48.0	48.0	48.1
CIFAR→SF		51.1	51.0	51.0	51.0	51.0
STL→CIFAR	75.0	74.1	74.1	74.1	74.1	74.1
STL→SF		76.2	76.2	76.2	76.2	76.2

Table 7: Results on CIFAR-10 and STL dataset in semi-supervised settings. SF is source fiction. The top table presented results for the settings with the 10 known labels for each class in the target domain, and the bottom table presents the result with the 100 known labels for each class